ELSEVIER

Earth and Planetary Science Letters 152 (1997) 1–9

EPSL

evidence for the Earth's most northerly volcanic activity

R. Mühe [a,*], H. Bohrmann [a], D. Garbe-Schönberg [a], H. Kassens [b]

[a] *Geologisch–Paläontologisches Institut und Museum der Universität, Olshausenstrasse 40, D-24159 Kiel, Germany*
[b] *Geomar Forschungszentrum für marine Geowissenschaften, Wischhofstrasse 1–3, D-24148 Kiel, Germany*

Received 15 April 1997; revised 27 August 1997; accepted 6 September 1997

Abstract

During the ARCTIC '91 expedition aboard RV *Polarstern* (ARK VIII/3) to the Central Arctic Ocean, a box corer sample on the Gakkel Ridge at 87°N and 60°E yielded a layer of sand-sized, dark brown volcanic glass shards at the surface of the sediment core. These shards have been investigated by petrographic, mineralogical, geochemical and radiogenic isotope methods. The nearly vesicle-free and aphyric glass shards bear only minute microphenocrysts of magnesiochromite and olivine (Fo_{88-89}). Most glasses are fresh, although some show signs of incipient low-temperature alteration. From their shapes and sizes, the glass shards most likely formed by spalling of glassy rinds of a nearby volcanic outcrop. Geochemically, the glasses are relatively unfractionated tholeiites with E-MORB trace element compositions. Thus, they are quite similar to the previously investigated ARK IV/3-11-370-5 basalts from 86°N [1].

The Nd and Sr isotopic ratios of PS 2167-2 glasses are significantly lower than for ARK IV/3-11-370-5 basalts and suggest an isotopically heterogeneous mantle source of Gakkel Ridge MORB between 86° and 87°N. The positive Δ-8/4 Pb value ($\sim$16) and high $^{87}Sr/^{86}Sr$ ratio (0.70270), found for PS 2167-2 glasses are similar to that of ARK IV/3-11-370-5 basalts and show the influence of the DUPAL isotopic anomaly in the high Arctic mantle. These results argue against the presence of an 'anti-DUPAL anomaly' in the mantle below the North Pole region and simple models of whole-mantle convection. © 1997 Elsevier Science B.V.

Keywords: mid-ocean ridge basalts; Arctic Ocean; Mid-Arctic Ocean Ridge; mineralogy; geochemistry; isotope ratios

1. Introduction

The Gakkel Ridge (Fig. 1), situated in the Eurasian Basin of the Arctic Ocean, is one of the least known active mid-oceanic ridges of the world. The ridge is the northern continuation of the Mid-Atlantic Ridge, separating the Eurasian from the Amerasian Plate. It is ca. 1800 km long, extending from 82°N 2°W to 80°N 125°E, and has formed since the Paleocene (magnetic anomalies 25/24 [2,3]). Due to the proximity of the pole of rotation at 68°N 137°E [4], the Gakkel Ridge has one of the slowest spreading rates of all mid-oceanic ridges (0.8–1.5 cm/yr; [5]), and shows high relief intensity and rift valley depths of more than 5000 m [6–9]. To date, perennial sea ice coverage of the Arctic Ocean has restricted hard rock sampling of the Gakkel Ridge to RV *Polarstern* cruise ARK IV/3 in 1987 [8]. The rocks recovered from the southern slope of the rift valley (ca. 30°E

* Corresponding author. Fax: +49 431 880 4376. E-mail: muehe@gpi.uni-kiel.de

PII S0012-821X(97)00152-0

longitude) are primitive basalts of early Quaternary age (i.e., perhaps less than 1 Ma old [10,1]).

During the ARCTIC '91 expedition in 1991 [11], RV *Polarstern* crossed the Gakkel Ridge at 60°E. The box corer PS 2167-2, located 4425 mbsl in the rift valley at 86° 56.1′N and 59° 4.5′E, recovered 42 cm of siliciclastic greyish-brown sandy to silty clay. These sediments were covered by a 1–2 mm thick layer of sand-sized dark brown volcanic glass shards. Neither in downcore sediments of station PS 2167-2, nor in any of the 50 other sediment sampling stations of the ARCTIC '91 expedition (including the four stations next to PS 2167-2 sampled higher above the ridge) was such a volcanic glass shard layer found.

Results of petrographic, geochemical and radiogenic isotope investigations of these glass shards are presented in this paper. Since these glasses constitute only the second sample of volcanic origin from the entire Gakkel Ridge, the data may improve our knowledge of magmatism at the world's least-studied mid-oceanic ridge and on the composition and dynamics of the mantle below the northern polar region.

2. Regional setting

The location of PS 2167-2 (86° 56.1′N and 59° 4.5′E, 4425 mbsl) is close to the major change in axial linearity of the Gakkel Ridge at its northernmost trend (Fig. 1). The regional half-spreading rate is between 0.5 and 0.6 cm/yr and it shows no

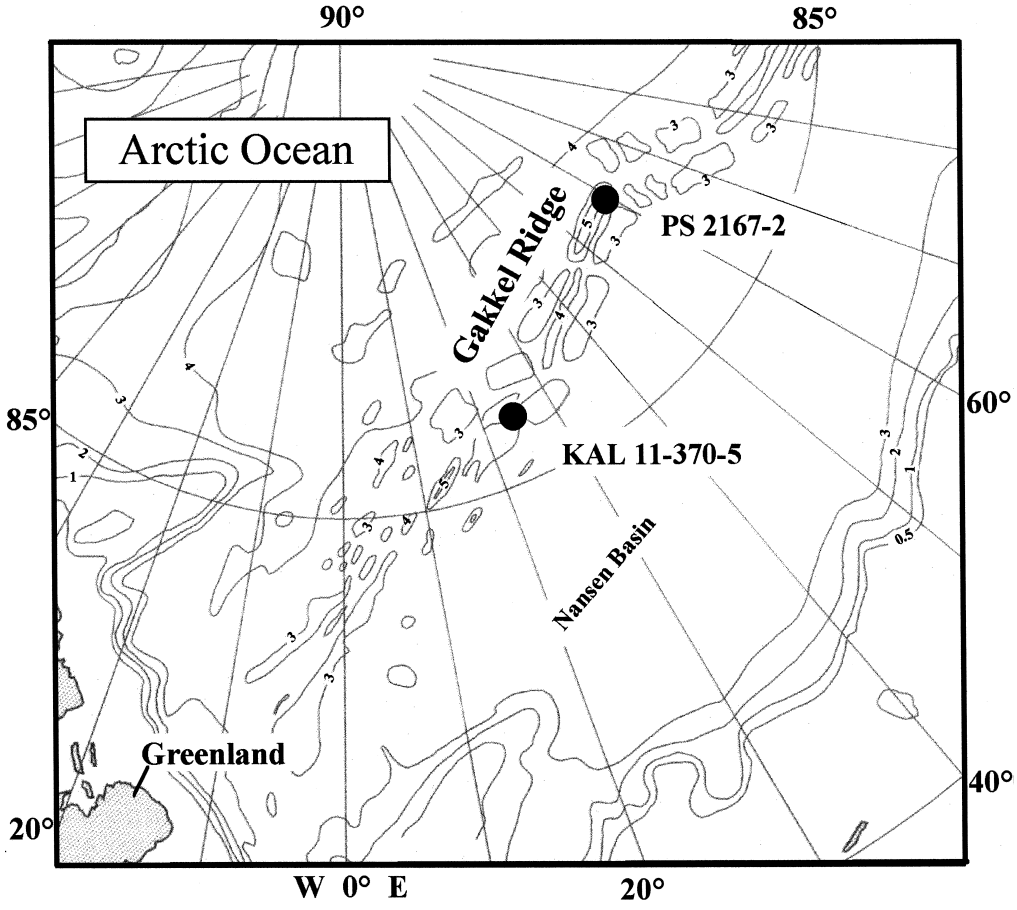

Fig. 1. Bathymetric sketch map of the Eurasian Arctic Ocean showing the Gakkel Ridge sampling areas of cruises ARK IV/3 (KAL 11-370-5) and ARK VIII/3 (PS 2167-2). Water depths in kilometres. The distance between the two sampling locations is ca. 270 km.

spreading obliquity [9]. The depth difference between the rift valley shoulder and floor is amongst the highest of the entire Gakkel Ridge (3400 m). This is due to the elevated feature at a distance of about 20 km on the southern ridge shoulder reaching 1100 mbsl (cf, [11,12]), that marks the locus of a major change in axial linearity of the ridge. The maximum slope inclination is 11° [11], resembling the values (8–12°) given by Bohrmann [7] at the 30°E ridge crossing during cruise ARK IV/3 (1986). From the cruise ARK IV/3 [13] and ODEN '91 [14] findings, it can be inferred that bottom water temperature is close to −1°C and the water current direction is parallel to the ridge axis. The PS 2167-2 glass shards were recovered at the north-facing foot of the southern ridge shoulder within the central rift valley, at 60°E longitude, within about 1 km of the rift axis. The site is elevated 75 m above the deepest portion of the regional valley floor (4500 m), and it is located 273 km east of where ARK IV/3 basalts (KAL 11-370-5) have been recovered [10,1].

3. Methods

A 0.5 cm section of the surface sediment was freeze dried, weighed and wet-sieved through a 63 μm sieve. The remaining > 63 μm material was split by sieving into various grain size classes and examined under a binocular microscope. Only glass shards showing no alteration (i.e., coatings of clay minerals, etc.) were separated by hand picking and ultrasonically cleaned in a mixture of distilled water and alcohol prior to analysis. Polished thin slides were prepared for microscopic and microprobe analyses of glass and mineral inclusions. Microprobe analyses were carried out with a 4-spectrometer Camebax microprobe (Cameca) and microprobe data was produced using techniques described in [10]. Major element analyses of 14 individual glass shards were determined. Usually 10 analyses (range 1–20) were performed for each shard and their average as well as standard deviations were calculated.

For determinations of trace element concentrations two aliquot samples (denoted PS 2167-2-a and PS 2167-2-b) were separately digested and analysed by inductively-coupled plasma mass-spectrometry. The techniques used are described in [1,15]. Sr, Nd and Pb isotopic compositions were determined at the Open University, Milton Keynes (P. Van Calsteren). Analytical procedures are described in [1].

For photo-documentation, scanning electron microscopy (SEM) was performed on a Cambridge Instruments CS 24 device of both Geomar and the Geological Department of the University of Kiel. Both instruments were equipped with an energy-dispersive X-ray analyser (EDX). Samples were sputtered with gold prior to analysis.

4. Results and discussion

4.1. Petrography, mineralogy and geochemistry

More than 90% of the sand-sized (> 63 μm) material consists of dark brown glass shards. A minor amount is mostly composed of planktonic foraminifers and other biogenic detritus [11]. Neither volcanic rock fragments nor separate mineral grains were observed.

The < 63 μm fraction was found to consist only of a minor amount of glassy material, mainly produced from breakage during sieving. The uppermost few millimetres of the sediment surface consist of 55.6% sand-sized material. In the > 63 μm fraction the following gravimetric grain size distribution was observed: > 1000 μm: 0.4%, 1000–500 μm: 5.4%, 250–500 μm: 47.5%, 125–250 μm: 32%, 63–125 μm: 14.7%. Thus, 80% of the glassy material occurs in the 125–500 μm grain size classes. The median grain size is about 250 μm.

In general, the glass shards display angular surfaces. Four different types can be distinguished. The most common are blocky and platy shards (Fig. 2a and b, respectively). Cuspate and strand-like types are very rare. Most shards display no vesicles, but a few show circular vesicles (< 1 vol.%; Fig. 2b) whose diameters do not exceed 70 μm.

Thin section study by transmitted light microscopy reveals that most shards are pure glass and do not show any crystal or signs of incipient devitrification. Only two of all shards investigated display minute crystals of octahedral brown spinel (< 50 μm) and of equant to skeletal olivines (< 100 μm).

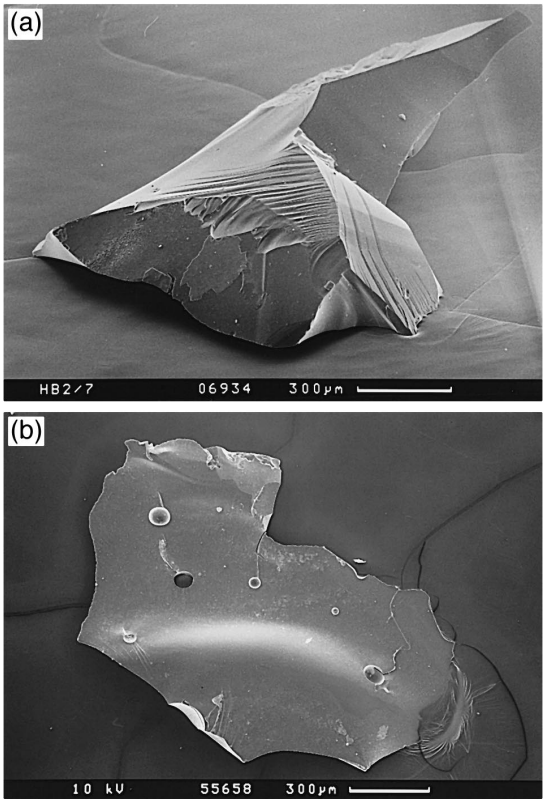

Fig. 2. SEM pictures of the two different types of fresh glass shards occurring in sample PS 2167-2. (a) Blocky, angular and vesicle-free type of glass shard, making up most of the glass particles of sample PS 2167-2. (b) Platy-type glass shard. Note small vesicles (<100 µm) on surface of shard.

Most glass shards studied under the binocular microscope appear fresh and are virtually unaltered. Occasionally, on surfaces of a few shards, whitish to greyish thin coatings typical of incipient smectite formation are observed.

4.2. Spinels

Three different spinel crystals were analysed by microprobe (Table 1). Cr_2O_3 contents in spinels vary from 32 wt% to 36 wt% and are negatively correlated with Al_2O_3 contents (30–26 wt%, respectively). $Cr/(Cr + Al)$ is in the range of 0.42–0.47. Both, FeO^* (18–19 wt%) and MgO (15.4–16 wt%) show only little variation. Spinels are classified as magnesiochromites or chromium spinels [16].

Fe^{3+}/Fe^{2-} ratios were recalculated based on stoichiometry and are in the range 0.33–0.45 (Table 1). $Mg/(Mg + Fe^{2-})$ exhibits very little variation (0.69–0.71). No significant chemical variation is seen in core and rim analyses of single crystals. The absence of zonation may be the result of low degrees of fractional crystallization of host lava and/or due to the absence of magma mixing or wall rock assimilation [17].

Spinels from samples ARK IV/3-11-370-5 [10] are higher in $Cr/(Cr + Al)$ (0.48–0.50), and this is probably due to slightly higher degrees of partial melting of their mantle source [18].

Table 1
Spinel analyses (wt%), from sample PS 2167-2 glass shards

	Grain No.			
	1		2	3
	Core	Rim	Core	Core
Oxides				
SiO_2	0	0	0	0
TiO_2	0.68	0.73	0.74	0.89
Al_2O_3	30.03	29.26	28.45	26.62
Fe_2O_3	4.91	5.12	5.39	6.13
FeO	14.47	14.15	13.19	13.64
MgO	15.94	16	16.03	15.41
MnO	0.17	0.14	0.11	0.16
CaO	0	0	0	0
Na_2O	0	0	0	0
K_2O	0	0	0	0
Cr_2O_3	32.41	33.17	33.77	36.06
NiO	0.41	0.08	0.8	0.17
Total	99.02	98.65	98.48	99.08
Oxygens	4	4	4	4
Cations				
Si	0	0	0	0
Ti	0.02	0.02	0.02	0.02
Al	1.06	1.04	1.02	0.96
Fe^{3+}	0.11	0.12	0.12	0.14
Fe^{2+}	0.32	0.31	0.29	0.31
Mg	0.71	0.72	0.72	0.7
Mn	0	0	0	0
Ca	0	0	0	0
Na	0		0	0
K	0	0	0	0
Cr	0.77	0.79	0.81	0.87
Ni	0.01	0	0.02	0
sum	3	3	3	3
$Cr/(Cr + Al)$	0.42	0.43	0.44	0.48
$Mg/(Mg + Fe^{2+})$	0.69	0.70	0.71	0.69

4.3. Olivines

Microprobe analyses of two individual olivine crystals are given in Table 2. Both olivines display fairly uniform forsterite contents (Fo_{88-89}), approaching mantle peridotite olivine compositions (Fo_{88-91}) [18]. NiO varies between 0.2 and 0.5 wt%. CaO is ca. 0.3 wt% and MnO values are ca. 0.2 wt%. As for spinels, no significant variation is seen between core and rim analyses of a single olivine crystal.

For comparison, olivines from sample ARK IV/3-11-370-5 display somewhat lower forsterite contents (Fo_{85-87}).

4.4. Major elements

Two representative major element analyses of glass shards (analyses A and B) are given in Table 3. Analysis A represents the major element chemistry seen in the majority (12) of the 14 glass shards analysed by microprobe, whereas B represents the major element chemistry of the remaining two glass shards analysed. Totals for analyses were generally in the range of 97–99 wt%, probably due to a certain amount of volatile phases (H_2O, CO_2, etc.) present in the glasses.

In terms of its MgO, Na_2O and K_2O contents, analysis A represents the most primitive and analysis B the most evolved major element chemistry of all analyses performed. However, analysis B values can be derived from analysis A values by fractionation of only 1–2% olivine (Fo_{88-89}) and Ca-rich plagioclase.

All PS 2167-2 glasses are hypersthene-normative olivine tholeiites (Table 3), as are the ARK IV/3-11-370-5 rocks. Applying the TAS classification scheme of [19] the PS 2167-2 glasses plot in the low-K subalkaline tholeiite field.

With regard to their major element chemistry, the PS 2167-2 glasses are fairly primitive MORB with MgO contents of nearly 9 wt%, which is quite similar to ARK IV/3-11-370-5 basalts [1]. Both, ARK IV/3-11-370-5 and PS 2167-2 samples show high Na_2O contents (>3 wt%). This is consistent with Klein and Langmuir's [20] model, which claims these lavas were erupted at extreme depth (>4400 m water depth) and at the ultra slow spreading rate of the Gakkel Ridge (1 cm/yr).

4.5. Trace elements

Results of trace element analyses are given in Table 4. In order to control analytical precision two aliquot samples (PS 2167-2-a and PS 2167-2-b) were measured. The primitive character of the PS 2167-2 glasses as seen in their major elements and their mineralogical record is also expressed in high Ni and Cr concentrations (165 μg/g and 300 μg/g). Mantle-incompatible elements are enriched and are com-

Table 2
Olivine analyses (wt%), from sample PS 2167-2 glass shards

Oxides	Grain No.									
	1				2					
	Rim	Rim	Core	Core	Core	Core	Core	Core	Rim	Rim
SiO_2	40.85	40.92	40.39	40.23	40.07	40.39	40.14	40.11	40.67	40.36
TiO_2	0	0	0	0	0	0	0	0	0	0
Al_2O_3	0	0	0	0	0	0	0	0	0	0
FeO	11.88	10.98	10.81	10.97	11.7	11.80	11.78	11.88	11.94	11.91
MgO	47.70	48.43	48.21	48.01	47.63	47.83	47.83	47.70	47.58	47.82
MnO	0.20	0.17	0.18	0.13	0.22	0.19	0.23	0.20	0.19	0.22
CaO	0.28	0.24	0.32	0.30	0.30	0.30	0.28	0.28	0.31	0.31
Na_2O	0	0	0	0	0	0	0	0	0	0
K_2O	0	0	0	0	0	0	0	0	0	0
NiO	0.27	0.35	0.20	0.17	0.34	0.23	0.45	0.39	0.49	0.31
sum	101.18	101.09	100.11	99.81	100.26	100.74	100.71	100.56	101.18	100.93
Fo	89	89	89	89	88	88	88	88	87	88

Table 3
Representative major element analyses (wt%) of sample PS 2167-2 glass shards [a] and CIPW normative minerals

Oxides		A	B	STD [b]
SiO_2		49.67	49.87	1%
TiO_2		1.41	1.64	3%
Al_2O_3		15.04	15.03	3%
FeO [c]		8.41	8.86	2%
MgO		8.77	7.69	1%
MnO		0.15	0.15	20%
CaO		11.33	11.00	1%
Na_2O		3.16	3.36	3%
K_2O		0.27	0.35	4%
Sum		98.21	97.95	
CIPW norm (wt%)				
or		1.61	2.09	
ab		26.97	28.74	
an		26.28	25.17	
hy	en	9.09	0.53	
	fs	0	0.32	
di	wo	12.70	12.53	
	en	10.97	7.39	
	fs	0	4.51	
ol	fo	1.38	8.02	
	fa	0	5.39	
mt		0.92	2.17	
hm		7.37	0	
il		2.70	3.15	
Sum		99.99	100.00	

[a] Analysis A represents the most primitive, analysis B the most evolved chemistry of all analyses (#109). 14 individual glass shards were subjected to microprobe analyses. Between 4 and 20 analyses were carried out on each individual shard.
[b] Standard deviations (STD) were calculated for analyses of individual grains (n = 12 for A, n = 2 for B). Only highest STD values are given.
[c] FeO calculated as 85% Fe^{3+} for CIPW norms.

parable to E-MORB [21]. Chondrite-normalized rare earth element (REE) patterns (Fig. 3) are nearly parallel to those of basalt samples 11-370-5 of 86°N but concentrations of REE are higher for sample PS 2167-2. Light rare earth element (LREE) enrichment of sample PS 2167-2 is indicated by the $(La/Sm)_N$ ratio of 1.09, which is slightly higher (1.03) than the samples 11-370-5 [1]. Similarly, the ratio of heavy REE $(Gd/Yb)_N$ is higher for sample PS 2167-2 (1.33) than for 11-370-5 (1.31). The comparably high $(Gd/Yb)_N$ ratio of both Gakkel Ridge samples indicates the possible presence of garnet in their mantle sources (see also [1]).

In general, most mantle incompatible element concentrations (except for Ba and Nb) are higher in sample PS 2167-2 than in sample 11-370-5. This could be due to: (1) slightly lower degrees of partial melting of a similar mantle source for PS 2167-2 than for 11-370-5 or (2) the source of PS 2167-2

Table 4
Trace elements (μg/g) and isotopic ratios [a]

	PS 2167-2-a	PS 2167-2-b
Li	4.99	5.03
Sc	33.6	36.5
V	272	280
Cr	271	325
Co	42.0	42.0
Ni	167	164
Cu	65.1	63.8
Zn	62.6	62.5
Ga	16.3	16.2
Rb	3.25	3.18
Sr	222	220
Y	29.2	28.9
Zr	116	116
Nb	6.41	6.35
Ba	43.1	43.0
La	6.39	6.45
Ce	16.4	16.5
Pr	2.53	2.55
Nd	12.3	12.3
Sm	3.76	3.73
Eu	1.35	1.37
Gd	4.47	4.48
Tb	0.797	0.792
Dy	4.96	5.00
Ho	1.05	1.06
Er	3.02	3.05
Tm	0.427	0.429
Yb	2.78	2.78
Lu	0.412	0.417
Hf	2.94	2.94
Ta	0.405	0.407
Pb	0.842	0.868
Th	0.440	0.443
U	0.203	0.207
$^{87}Sr/^{86}Sr$		0.70270 (2)
$^{143}Nd/^{144}Nd$		0.512996 (21)
$^{206}Pb/^{204}Pb$		18.085 (19)
$^{207}Pb/^{204}Pb$		15.422 (17)
$^{208}Pb/^{204}Pb$		37.652 (58)
Δ-Sr		27
Δ-7/4		−2.94
Δ-8/4		16.02

[a] Analyst: P. Van Calsteren at the Open University, Milton Keynes.

basalts is slightly more enriched in incompatible elements than the mantle source of 11-370-5. Based on the lower Cr/(Cr + Al) ratios found in spinels of the PS 2167-2 than in 11-370-5 glasses, an origin with a slightly lower degree of partial melting [18] is indicated. However, different mantle sources are suggested by the isotopic data.

4.6. Sr, Nd, and Pb isotopic ratios

Sr, Nd, and Pb isotopic ratios of PS 2167-2 glass shards are also given in Table 4. Especially the Nd, but also the Sr isotopic ratios of PS 2167-2 glass shards (0.512996 and 0.70270, respectively) are significantly lower than for ARK IV/3-11-370-5 basalt samples (0.513154 and 0.70284 (sample 3), respectively) from 86°N (Fig. 4). These differences mark a clear change in the isotopic composition of the Arctic mantle between 86° and 87°N and suggest the Arctic mantle to be heterogeneous over this distance.

In a recent paper investigating the radiogenic isotope composition of the high latitude North Atlantic mantle, Mertz and Haase [22] point out that between 34°N and ''at least 86°N'' MORB samples fall into the ''radiogenic Sr group'' suggested by Schilling and co-workers [23]. The isotopic composition of sample PS 2167-2 suggests that basalts belonging to the ''radiogenic Sr group'' [23] do not occur north of 86° in the Arctic.

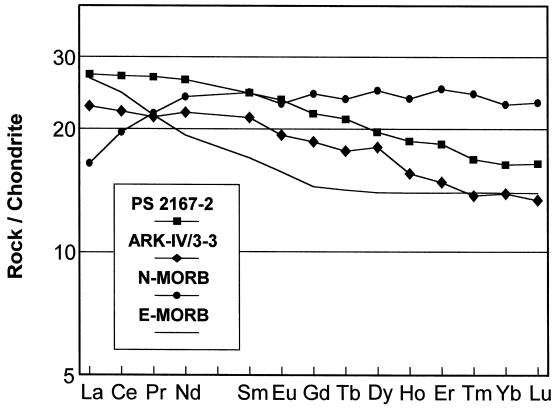

Fig. 3. Chondrite-normalized [21] rare earth element diagram. Sample PS 2167-2 (the averages of analyses given in Table 4 are used) is an E-MORB. Although displaying a similar pattern to sample ARK IV/3-3, which is also an E-MORB [1], sample PS 2167-2 has higher rare earth element concentrations. N-MORB and E-MORB patterns [30,21] are added for comparison.

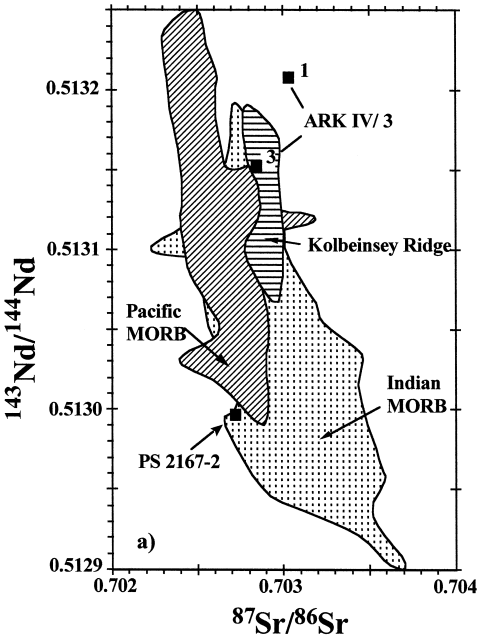

Fig. 4. $^{143}Nd/^{144}Nd$ versus $^{87}Sr/^{86}Sr$ compared to ratios of samples 1 and 3 from ARK IV/3-11-370-5 [1], and Pacific, Indian and Kolbeinsey Ridge MORB (data for fields are taken from the literature). Compared to ARK IV/3-11-370-5 basalts, sample PS 2167-2 displays more radiogenic $^{143}Nd/^{144}Nd$ and less radiogenic $^{87}Sr/^{86}Sr$ ratios, respectively.

A Δ-8/4 Pb value for PS 2167-2 glasses of 16.02 has been calculated according to the procedure of Hart [24] and is also given in Table 4. A positive Δ-8/4 Pb value and fairly high $^{87}Sr/^{86}Sr$ values are indicative of the influence of the DUPAL isotopic anomaly in MORB [25]. The Δ-8/4 Pb value for PS 2167-2 is slightly lower but still in the range of values found for the ARK IV/3 basalts. Therefore, these results strengthen previous arguments [1] that the DUPAL-tainted Gakkel Ridge basalts do not support the hypothesis of a polar 'anti-DUPAL anomaly' that might develop as a result of a whole-mantle convection, caused by equatorial upwelling of enriched material from the lower mantle and polar downwelling [24].

4.7. Origin of glass shards

Ocean-floor basalt origin is indicated by the chemical composition (Tables 3 and 4) of the glass

shards. A single eruption origin is inferred from the physical and chemical homogeneity of the glass shards.

The grain size and shape of the glass shards are thought to be controlled by the processes involved in the ''spalling of glassy crusts of pillows of sheet lavas during cooling contraction of the flow interior or expansion of growing pillow tubes'' [26]. The rarity of vesicles (Fig. 2b), which is caused by high hydrostatic pressure, preventing magma degassing, suggests that the glass shards were most likely formed in more than 4000 m water depth, well below the VFD (volatile fragmentation depth; [26]) and the critical pressure of seawater (about 3200 m water depth).

The absence of signs of wear and scratching on the shards and the lack of detrital compounds exclude reworking processes for the material. Considering that four nearby sampling stations, higher up the ridge shoulder, did not contain any glass shards, it is most likely that the site of eruption of the PS 2167-2 shards was very close.

There was no film of terrigenous or biogenic mud observed on the shards. Taking into account the currently slow sedimentation rates (< 1 cm/ky) encountered at the Gakkel Ridge [27–29], the deposition of the shard layer cannot be older than a few tens, at most a few hundreds, of years. Assuming higher sedimentation rates due to sediment focusing in the central rift valley [28], the age of deposition could be even younger. The very low degree of alteration seen on only a small number of glass shards also supports the idea that they are only a few tens or hundreds of years old.

5. Conclusions

The following conclusions were reached as a result of this study:

1. The glass shards from station PS 2167-2 comprise the first finding of fresh volcanic material from the Arctic Ocean floor. Its occurrence in the deep valley floor of the Gakkel Ridge proves recent volcanic activity at the world's most northerly and slowest spreading mid-ocean ridge.
2. According to grain size, shape, mineral content, and its primitive basaltic major element chemistry, the PS 2167-2 glasses most likely originate from spalling of glassy pillow rinds or the chilled margins of sheet flow MORB lavas that erupted near site PS 2167-2.
3. The high percentage of fresh volcanic glass is evidence that the shards are of Recent age, probably not older than a few hundred years.
4. An origin from a single tholeiitic eruption at the Gakkel Ridge is inferred from the major element chemistry of individual shards. Geochemically, the PS 2167-2 glasses are E-MORB, similar to the ARK IV/3-11-370-5 basalts, but with somewhat higher concentrations for most trace elements.
5. The distinctly lower Nd and Sr isotopic ratios of PS 2167-2 glasses in comparison to those of ARK IV/3-11-370-5 basalts indicate mantle heterogeneity and a change in the isotopic composition of the Arctic mantle between 86°N and 87°N.
6. With a positive Δ-8/4 Pb value of ~ 16 and high $^{87}Sr/^{86}Sr$ (0.70270), the PS 2167-2 glasses show the influence of the DUPAL isotopic anomaly in their mantle source. These results support previous arguments [1] against the presence of an 'anti-DUPAL anomaly' in the mantle below the North Pole region and Hart's [24] model of whole-mantle convection.

Acknowledgements

Technical assistance with analyses from P. Van Calsteren, Milton Keynes, U.K. (Sr, Nd and Pb isotopes), D. Ackermand and B. Mader (microprobe) and T. Arpe (ICP–MS) is gratefully acknowledged. We are grateful to R. Spielhagen for providing the samples. We thank C.W. Devey for helpful comments on an earlier version of the manuscript. We are particularly grateful to R. Batiza, B. Hanan and an anonymous reviewer for their thoughtful and careful reviews of the manuscript. Furthermore, we wish to thank the crew of the RV *Polarstern* for their logistic support during the ARCTIC '91 expedition. The research was funded by the German Ministry for Research and Technology (FZK 525 4003 03 R409A). ***[FA]***

References

[1] R. Mühe, C.W. Devey, H. Bohrmann, Isotope and trace element geochemistry of MORB from the Nansen–Gakkel ridge at 86° north, Earth Planet. Sci. Lett. 120 (1993) 103–109.

[2] P.R. Vogt, C. Bernero, L.C. Kovacs, P. Taylor, Structure and plate tectonic evolution of the Marine Arctic as revealed by aeromagnetics, Oceanol. Acta Spec. Publ. (1981) 25–40.

[3] S.P. Srivastava, Evolution of the Eurasian Basin and its implications to the motion of Greenland along Nares Strait, in: E.S. Husebye, G.L. Johnson, Y. Kristoffersen (Eds.), Geophysics of the Polar Regions, reprinted from Tectonophysics 114, Elsevier, Amsterdam, 1985, pp. 29–53.

[4] W.C. Pitman, M. Talwani, Seafloor spreading in the North Atlantic, Geol. Soc. Am. Bull. 83 (1972) 646–691.

[5] Y. Kristoffersen, The Nansen Ridge, Arctic Ocean; some geophysical observations of the rift valley at slow spreading rate, Tectonophysics 89 (1982) 161–172.

[6] N. Subow, Die wissenschaftliche Bedeutung der Sedowdrift, in: K. Badigin, N. Subow (Eds.), Im Eis der Arktis, SWA Verlag, Berlin, 1946, pp. 148–170.

[7] H. Bohrmann, Morphology and Geological Record of the Nansen–Gakkel Ridge near 86°N (Arctic Ocean), Abstr. ARWAWC: Geologic History of the Polar Oceans: Arctic versus Antarctic, Bremen, 1988.

[8] J. Thiede, Scientific cruise report of Arctic Expedition ARK IV/3, Rept. Polar Res. 43 (1988) 263.

[9] O. Eldholm, A.M. Karasik, P.A. Reksnes, The North American Plate boundary, in: A. Grantz, L. Johnson, J.F. Sweeney (Eds.), The Arctic Ocean Region, Vol. L, Geol. Soc. Am., Boulder, CO, 1990, pp. 171–184.

[10] R. Mühe, H. Bohrmann, P.K. Hörmann, J. Thiede, P. Stoffers, Spinifex basalts with komatiite–tholeiite trend from the Nansen–Gakkel Ridge (Arctic Ocean), Tectonophysics 190 (1991) 95–108.

[11] Shipboard Scientific Party, D.K. Fütterer, ARCTIC-91: The Expedition ARK-VIII/3 of RV ''Polarstern'' in 1991, Rept. Polar Res. 107 (1992) 267.

[12] R.K. Perry, H.S. Fleming, J.R. Weber, Y. Kristoffersen, J.K. Hall, A. Grantz, G.L. Johnson, Bathymetry of the Arctic Ocean, bathymetric chart 1.49 m by 1.06 m, scale 1:4,704,075, Naval Res. Lab., Washington, 1985.

[13] L.G. Anderson, E.P. Jones, K.P. Koltermann, J.H. Swift, D.W.R. Wallace, The first oceanographic section across the Nansen Basin in the Arctic Ocean, Deep Sea Res. 36 (3) (1989) 475–482.

[14] L.G. Andersen, G. Björk, O. Holby, E.P. Jones, G. Kattner, K.P. Koltermann, B. Liljeblad, R. Lindegren, B. Rudels, J. Swift, Water masses and circulation in the Eurasian Basin: Results from the ''Oden 91'' expedition, J. Geophys. Res. 99 (C2) (1994) 3273–3283.

[15] C.-D. Garbe-Schönberg, Simultaneous determinations of 37 trace elements in 28 international rock standards by ICP–MS, Geostand. Newsl. XVII (1993) 81–97.

[16] H. Sigurdsson, Spinels in leg 37 basalts and peridotites: Phase chemistry and zoning, Init. Rept. Deep Sea Drill. Proj. 37 (1977) 883–891.

[17] J.F. Allan, R.O. Sack, R. Batiza, Cr-rich spinels as petrogenetic indicators: MORB-type lavas from the Lamont seamount chain, eastern Pacific, Am. Mineral. 73 (1988) 741–753.

[18] H.J.B. Dick, T. Bullen, Chromian spinel as a petrogenetic indicator in abyssal and alpine-type peridotites and spatially associated lavas, Contrib. Mineral. Petrol. 86 (1984) 54–76.

[19] R.W. LeMaitre (Ed.), A Classification of Igneous Rocks and Glossary of Terms, Blackwell Scientific, Oxford, 1989, 193 pp.

[20] E.M. Klein, C.H. Langmuir, Global correlations of ocean ridge basalt chemistry with axial depth and crustal thickness, J. Geophys. Res. 92 (1987) 8089–8115.

[21] S.-S. Sun, W.F. McDonough, Chemical and isotopic systematics of oceanic basalts: implications for mantle composition and processes, in: A.D. Saunders, M.J. Norry (Eds.), Magmatism in Ocean Basins, Geol. Soc. London Spec. Publ. 42 (1989) 313–345.

[22] D.F. Mertz, K.M. Haase, The radiogenic isotope composition of the high-latitude North Atlantic mantle, Geology (in press).

[23] J.-G. Schilling, B.B. Hanan, B. McCully, R.H. Kingsley, D. Fontignie, Influence of the Sierra Leone mantle plume on the equatorial Mid-Atlantic Ridge: A Nd–Sr–Pb isotopic study, J. Geophys. Res. 99 (1994) 12005–12028.

[24] S.R. Hart, A large scale isotope anomaly in the Southern Hemisphere mantle, Nature 309 (1984) 753–757.

[25] P. Castillo, The Dupal anomaly as a trace of the upwelling lower mantle, Nature 336 (1988) 667–670.

[26] R.V. Fisher, H.-U. Schmincke, Pyroclastic Rocks, Springer, Heidelberg, 1984, 472 pp.

[27] H. Bohrmann, R. Botz, P. Stoffers, J. Thiede, Excess ^{230}Th profiles of long sediment cores from the Arctic Ocean: Evidence for the slow sedimentation rates from the western Nansen–Gakkel Ridge near 86°N, Abstr. 28th Int. Geol. Congr., Washington, D.C., vol. 1, 1989, p. 161.

[28] H. Bohrmann, Radioisotope stratigraphy, sedimentology and geochemistry of Late Quaternary sediments from the Eastern Arctic Ocean, Rept. Polar Res. 9 (1991) 133.

[29] R. Stein, C. Schubert, C. Vogt, D.K. Fütterer, Stable isotopes stratigraphy, sedimentation rates, and salinity changes in the Latest Pleistocene to Holocene eastern central Arctic Ocean, Mar. Geol. 119 (1994) 333–355.

[30] A.W. Hofmann, Chemical differentiation of the Earth: the relationship between mantle, continental crust and oceanic crust, Earth Planet. Sci. Lett. 90 (1988) 297–314.